Journal of Hazardous Materials 192 (2011) 1572–1579

Contents lists available at ScienceDirect

Journal of Hazardous Materials

journal homepage: www.elsevier.com/locate/jhazmat

Low toxicity of HfO_2, SiO_2, Al_2O_3 and CeO_2 nanoparticles to the yeast, *Saccharomyces cerevisiae*

Citlali García-Saucedo*, James A. Field, Lila Otero-Gonzalez, Reyes Sierra-Álvarez

Department of Chemical and Environmental Engineering, University of Arizona, P.O. Box 210011, Tucson, AZ, USA

ARTICLE INFO

Article history:
Received 2 February 2011
Received in revised form 26 June 2011
Accepted 28 June 2011
Available online 2 July 2011

Keywords:
Alumina
Ceria
Cytotoxicity
Hafnia
Nanotoxicology
Silica
Yeast

ABSTRACT

Increasing use of nanomaterials necessitates an improved understanding of their potential impact on environment health. This study evaluated the cytotoxicity of nanosized HfO_2, SiO_2, Al_2O_3 and CeO_2 towards the eukaryotic model organism *Saccharomyces cerevisiae*, and characterized their state of dispersion in bioassay medium. Nanotoxicity was assessed by monitoring oxygen consumption in batch cultures and by analysis of cell membrane integrity.

CeO_2, Al_2O_3, and HfO_2 nanoparticles were highly unstable in yeast medium and formed micron-sized, settleable agglomerates. A non-toxic polyacrylate dispersant (Dispex A40) was used to improve nanoparticle stability and determine the impact of enhanced dispersion on toxicity. None of the NPs tested without dispersant inhibited O_2 uptake by yeast at concentrations as high as 1000 mg/L. Dispersant supplementation only enhanced the toxicity of CeO_2 (47% at 1000 mg/L). Dispersed SiO_2 and Al_2O_3 (1000 mg/L) caused cell membrane damage, whereas dispersed HfO_2 and CeO_2 did not cause significant disruption of membrane integrity at the same concentration. These results suggest that the O_2 uptake inhibition observed with dispersed CeO_2 NPs was not due to reduced cell viability. This is the first study evaluating toxicity of nanoscale HfO_2, SiO_2, Al_2O_3 and CeO_2 to *S. cerevisiae*. Overall the results obtained demonstrate that these nanomaterials display low or no toxicity to yeast.

1. Introduction

Nanoparticles (NPs) are characterized by having less than 100 nm in size in more than one dimension. The unique properties of many engineered nanomaterials and their enormous potential in a variety of applications, such as drug delivery systems, electronic circuits, catalysts, and agents for environmental remediation [1,2], has lead to a sharp increase in the industrial production of engineered nanomaterials (ENMs) in recent years [3–5]. The nanotechnology sector has achieved a multibillion US$ market, and is expected to grow to 1 trillion US$ by 2015 [6].

Inorganic oxide NPs, including those of silica (SiO_2), alumina (Al_2O_3), and ceria (CeO_2), are among the most commonly utilized ENMs, and the three oxides are included in the Organization for Economic Cooperation and Development's (OECD) priority list of ENMs requiring urgent testing for human health and environmental safety [7]. These nanomaterials are widely used as abrasives in chemical-mechanical planarization processes in semiconductor manufacturing [8]. Nanoscale SiO_2 has also great importance in the fabrication of electric and thermal insulators, catalyst supports, and it is used as an adsorbent and filler material [9]. Nano-sized CeO_2 is utilized in automobile catalytic converters, and as a fuel additive to promote combustion [10]. Hafnium oxide (HfO_2) is an emerging ENM being considered for application in immersion photolithography [11,12].

The rapid increase in the utilization and environmental emissions of ENMs has been accompanied by a growing concern among scientists and regulatory agencies about their potential negative impact on human health and the environment. Studies conducted over the past 10 years have provided interesting evidence that a variety of ENMs, including metal oxides, fullerenes, and carbon nanotubes, can cause toxic effects to mammalian cells [13–15] and other living organisms [16–18]. Although the mechanisms of ENM toxicity are poorly understood, numerous reports suggest that the toxicity exhibited by some nanomaterials might be related to their small dimensions that allow these materials to enter into eukaryotic cells and have high surface reactivity, and/or ability to release biocidal species, among others [14,19–21].

Although numerous nanotoxicity studies have been published in recent years, most of the experiments carried out so far have not adequately characterized NPs with regard to their chemical composition and physicochemical properties [22]. Accurate evaluation of ENM toxicity requires comprehensive material characterization

* Corresponding author. Tel.: +1 520 626 2896; fax: +1 520 621 6048.
E-mail address: citla_2000@yahoo.com (C. García-Saucedo).

0304-3894/$ – see front matter © 2011 Elsevier B.V. All rights reserved.
doi:10.1016/j.jhazmat.2011.06.081

because the toxicity of NPs appears to depend on several factors including particle size, particle morphology, particle composition, surface area, and surface chemistry [15,23,24]. Characterization of the aggregation behavior and size of NPs in the bioassay medium is also critical because many nanomaterials form large aggregates in aqueous systems. This agglomeration raises concerns when considering size-dependent toxicity, specific surface area toxicity, and dose-dependent toxicity for in vitro experiments [15,25], and it complicates the interpretation of data obtained in toxicity studies.

The yeast *Saccharomyces cerevisiae* is frequently used in toxicological evaluations of chemicals such as heavy metals, anti-cancer drugs, herbicides, among others [26–28]. *S. cerevisiae* is one of the unicellular eukaryotic model organisms most studied in molecular and cell biology because its cellular structure and functional organization share many similarities with cells in plants and animals. Another advantage of using yeast is its short generation time and easy cultivation. Surprisingly, the cytotoxicity of NPs to yeast is still poorly understood and very few toxicity studies have considered the impact of NPs on *S. cerevisiae* and other yeast species. We are only aware of three studies of nanotoxicity that have used *S. cerevisiae* as a model organism [29–31]. The nanomaterials evaluated in those studies included ZnO, CuO, TiO_2, iron oxides, and fullerene.

The main objective of this study was to evaluate the toxicity of widely utilized inorganic oxide NPs (SiO_2, Al_2O_3 and CeO_2) and an emerging ENM, HfO_2, towards *S. cerevisiae*, and to characterize their particle size and state of dispersion in the culture medium. Cytotoxicity was measured with O_2-consumption and membrane integrity assays. The impact of a dispersants used to stabilize NPs in the culture medium was also evaluated.

2. Materials and methods

2.1. Nanoparticles

Al_2O_3 (50 nm, 99% purity) and CeO_2 (50 nm, 99.95%) were obtained from Sigma–Aldrich (St. Louis, MO). SiO_2 (10–20 nm, 99.5%) and HfO_2 (100 nm, 99.9%) were purchased from American Elements (Los Angeles, CA). All nanomaterials were supplied as a dry powder.

2.2. Preparation of suspensions

NP stock dispersions (4000 mg/L) were prepared in filtered (0.45 μm) nanopure water (Millipore, resistivity > 18.2 MΩ/cm). Dispersions were sonicated (DEX® 130, 130 Watts, 20 kHz, Newtown, CT) at 70% amplitude during 5 min. In some experiments, NP stock dispersions containing 400 mg/L of the ammonium polyacrylate dispersant, Dispex A40 (BASF, Freeport, TX) were utilized to minimize NP aggregation. The pH of the NP stocks was adjusted to 6.50 using diluted HCl or NaOH, as required. Stocks were stored at 4 °C and used within 24 h of preparation. All stocks were sonicated for 5 min before use.

2.3. Batch toxicity bioassays

Bioassays were performed in 160 mL serum bottles (Wheaton, Millville, NJ) containing 25 mL of liquid medium. The pH-6.50 yeast extract peptone dextrose (YEPD) basal medium utilized consisted of glucose (1.7 g/L), peptone (1.7 g/L), and yeast extract (0.84 g/L), which. is equivalent to approximately 5 gram theoretical oxygen demand (ThOD) per liter. Flasks were spiked with aliquots of the NP stock to obtain final concentrations of 100, 500 and 1000 mg/L of NPs. To evaluate the impact of NP dispersion on cytotoxicity, bioassays amended with known concentrations of NPs and a non-toxic dispersant (Dispex, 10:1, NP:Dispex, w/w) were also performed. Flasks lacking NPs served as uninhibited controls. Culture flasks were inoculated using 0.1% (w/w) of a commercial yeast preparation (*S. cerevisiae*, Rapid Rise Yeast, Fleischmann's, Oakville, ON, Canada), which provided an initial cell concentration of approximately 1×10^9 cells/mL. Subsequently, they were sealed with butyl rubber stoppers and crimp caps. Non-inoculated controls with/without NPs in YEPD medium were included to confirm lack of abiotic consumption of oxygen. Next, the flask headspace was flushed with $He/CO_2/O_2$ gas (60/20/20, v/v) for 6 min in order to provide 1.5 mmol of O_2 per flask. The ThOD concentration of the medium and O_2 addition were set to ensure O_2 depletion in the NP-free controls after 10–12 h. Nitrogen was excluded from the headspace to avoid interference with the chromatographic analysis of oxygen. The cultures were incubated at 30 °C in the dark for 10–14 h in an orbital shaker (200 rpm).

Headspace samples were obtained periodically from all flasks and they were analyzed for O_2 content. The maximum sO_2 consumption activities (mg O_2-consumed/(flask – h) were calculated from the slope of the O_2 content versus time graph, as the mean value of duplicate assays. In each case, the maximum activity at a given NP concentration was determined during the time period when the NP-free control displayed maximum activity. The inhibition of O_2 consumption observed was calculated as shown below:

$$\text{Inhibition}\,(\%) = 100 - \left[100\frac{\text{maximum activity at the tested concentration}}{\text{maximum activity of the control}}\right]$$

The initial concentration of NPs causing 50% reduction in activity compared to an uninhibited control was referred to as IC_{50}. These values were calculated by interpolation in the graph plotting the inhibition observed (expressed as percent) as a function of the inhibitor concentration.

2.4. Stability of nanoparticle dispersions

The stability of NP dispersions in the YEPD medium and in demineralized water (pH 6.5) was evaluated by determining the particle size distribution (PSD) and zeta potential of non-inoculated, cell-free samples following shaking (200 rpm) for 10 h at 30 °C. Additional information was obtained by allowing samples to settle for 30–45 min under static conditions, and analyzing samples of the supernatant for PSD, zeta potential, and the concentration of Si, Al, Hf, or Ce. All samples were collected in 15 mL conical polypropylene tubes BD Falcon™. Samples of the supernatant were collected carefully to avoid carryover of any settled material. PSD and zeta potential measurements were carried immediately after sampling. Samples for NP chemical analysis were acidified with a few drops of concentrated nitric acid and they were stored at 4 °C till analysis.

2.5. Particle size distribution and zeta potential measurements

The zeta potential of NPs dispersions was measured with a Zeta Sizer Nano ZS (Malvern, Inc., Sirouthborough, MA). The instrument utilizes the Smoluchowski equation to correlate particle electrophoretic mobility to zeta potential. PSD measurements were performed by dynamic light scattering (DLS) using the same instrument.

2.6. Transmission electron microscopy (TEM)

NPs were examined by transmission electron microscopy to gain information on particle morphology and size. TEM images were acquired on a Hitachi H8100 at 200 keV. NPs were suspended in

isopropanol and sonicated in a bath sonicator for 5 min and subsequently deposited onto lacey formvar/carbon-coated TEM 300 mesh copper grids before examination.

2.7. Flow cytometry

A commercial kit (*Funga*Light™, Invitrogen, Carlsbad, CA) was used to assess damage of the yeast cell membrane by NPs. The kit combines a cell-permeable esterase substrate (5-carboxyfluorescein diacetate, CFDA-AM) with a membrane integrity indicator (propidium iodide, PI) to evaluate the vitality of yeast cells by flow cytometry. Flow cytometry analyses were performed in a BD FACscan™ system (Becton-Dickinson Biosciences, San Jose, CA) by counting 10,000 events. The excitation source was a 15 mW argon laser tuned to 488 nm.

Yeast cells were exposed to NPs (1000 mg/L) amended with dispersant (100 mg Dispex/L) using the culture conditions described in the batch bioassays. NP-free controls with dispersant (100 mg/L) were run in parallel. Dispersion aliquots (1 mL) were collected after 10 h of incubation, diluted ten times with deionized (DI) water, prepared following the instructions provided by the kit manufacturer, and analyzed by flow cytometry 1 h after incubation with the dyes. Various controls were run in parallel, including NPs in non-inoculated YEPD medium, yeast in YEPD medium without dyes, yeast in YEPD medium with CFDA-AM, and killed yeast (0.5% sodium dodecylsulfate) in YEPD medium with PI. In the assay used, yeast cells stained fluorescent green are alive, while cells stained fluorescent red are dead cells showing membrane damage. Flow cytometry analysis of the nanosized oxides (1000 mg/L) in cell-free assays confirmed that NPs did not interfere with the assay as indicated by negligible counts of green or red-stained particles as compared to the inoculated samples.

2.8. Analytical methods

Prior to the determination of metal content, NP samples were subjected to microwave-assisted acid digestion (MSD2100, CEM Corp., Matthews, NC). Liquid samples (1 mL) were mixed with a suitable digestion solution (10 mL). CeO_2 samples were digested using 71% HNO_3 (8 mL) and 30–32% H_2O_2 (2 mL); HfO_2 samples with 49% HF (0.1 mL) and 37% HCl (9.9 mL); Al_2O_3 samples with 50% HCl (10 mL), and SiO_2 samples with 1% HF (10 mL). The digestion conditions for CeO_2 and HfO_2 were 30 min at 70 psi, for Al_2O_3 45 min at 70 psi, and for SiO_2 45 min at 70 psi. Digested samples were diluted, when needed, and they were supplemented with HNO_3 acid to a final concentration of 2% (v/v), with the exception of SiO_2 and HfO_2 samples that were supplemented with HF to a final concentration of 0.1% (v/v). The resulting solutions were measured by inductively coupled plasma-optimal emission spectroscopy (ICP-OES Optima 2100 DV, Perkin–Elmer TM, Shelton, CT). Hf, Si, Al, and Ce in digested samples were analyzed at a wavelength of 264.141, 251.611, 396.153 and 413.764 nm, respectively. The detection limits for HfO_2, SiO_2, Al_2O_3, and CeO_2 were 1, 10, 1 and 10 μg/L, respectively.

O_2 concentration in gas samples was analyzed in a gas chromatograph (HP5890, Agilent Technologies, Palo Alto, CA) fitted with a Carboxen-1010 Plot column (30 m × 0.32 mm, Supelco, St. Louis, MO) and a thermal conductivity detector. Measurements of pH were conducted according to standard methods [32].

3. Results and discussion

3.1. Physicochemical characterization of nanoparticles

Fig. 1 shows transmission electron micrographs obtained for CeO_2, HfO_2, SiO_2 and Al_2O_3. The figures indicate that the average particle size of each material is similar to the values reported by the manufacturers, *i.e.*, 50 nm for Al_2O_3 and CeO_2, 10–20 nm for SiO_2, and 100 nm for HfO_2. The micrographs also indicate that the particle morphology varied depending on the oxide, with spherical particles dominating in most samples. Needle-like particles were also observed in CeO_2 and Al_2O_3 samples. Transmission electron microscopy micrographs cannot provide an accurate representation of the aqueous NP dispersions in the culture medium because due to the high vacuum conditions in the transmission electron microscopy, the imaged NP suspensions were dry. Dynamic light scattering was utilized for evaluate particle size distribution in aqueous suspensions.

3.2. Nanoparticle aggregation in yeast culture medium

All the NPs evaluated in this study, with the exception of SiO_2, showed a high tendency to aggregate in yeast culture medium and, to a lesser extent in DI water at the same pH value of 6.5 (Fig. 2). Nano-sized CeO_2 and Al_2O_3 dispersions were strongly destabilized in the yeast culture medium as indicated by the very high light intensity averaged particle sizes determined, 3394 and 2237 nm, respectively. Dispersions of both inorganic oxides were also found to agglomerate in DI water (pH 6.5) although considerably less than in YEPD medium (Fig. 2). HfO_2 NPs tended to aggregate both in YEPD medium and water (pH 6.5) and the average particle diameter of both dispersions ranged from 1660 to 1760 nm (Fig. 2), which correspond to a 17- to 18-fold increase over the primary particle size (100 nm). These trends were confirmed by the very low concentrations of residual Al, Ce, and Hf present in the supernatant of samples dispersed in water (0.4, 4.0 and 60.2% of the initial concentration, respectively) or YEPD medium (only 2.5–3.2% of the initial content) (Fig. 3) after incubation for 10 h. These low recoveries indicate that large fractions of the inorganic oxides formed large size aggregates that settled out. Finally, SiO_2 dispersions appeared to be considerably more stable in both water and YEPD medium as shown by a moderate increase in the average particle diameter to 347 and 423 nm, respectively. The high stability of SiO_2 dispersions is also confirmed by the high recovery of Si determined in the supernatant of the DI water and yeast medium samples, 97.9 and 80.8% of the initial concentration, respectively.

The observed aggregation of HfO_2, Al_2O_3, and CeO_2 in circum-neutral water is not surprising since their isoelectric points (IEP) are in the pH region of natural waters (pH 6–8) [33,34]. At pH values close to their respective IEP, the three nanomaterials have low surface charge and the attractive forces between particles become sufficiently strong to promote NP aggregation. In contrast, SiO_2 has a very low IEP (1.7–3.5) [33] and, therefore, these NPs are expected to show a net negative charge over wide pH ranges. The high zeta potential value determined for SiO_2 dispersions in water (−41.2 mV) is in agreement with that hypothesis and could explain the relatively high stability of these dispersions. Nonetheless, SiO_2 exhibited a 28-fold increase over its primary size when dispersed into water, indicating some aggregation, although not enough for large-scale sedimentation. Previous studies have reported a similar behavior for dispersion of SiO_2 NPs in circum-neutral water [25].

The reduced stability observed for HfO_2, Al_2O_3, and CeO_2 dispersions in yeast culture medium when compared to the water samples is probably due to interaction of the NPs with organic components and salts in the YEPD medium. The state of NP dispersion is known to depend strongly on the type and content of organic matter and salts in the water. Particles can be stabilized or destabilized by organic compounds, including proteins which were present in the YEPD medium utilized in this study, and these effects will depend on the IEP of the NP, the charge and molecular

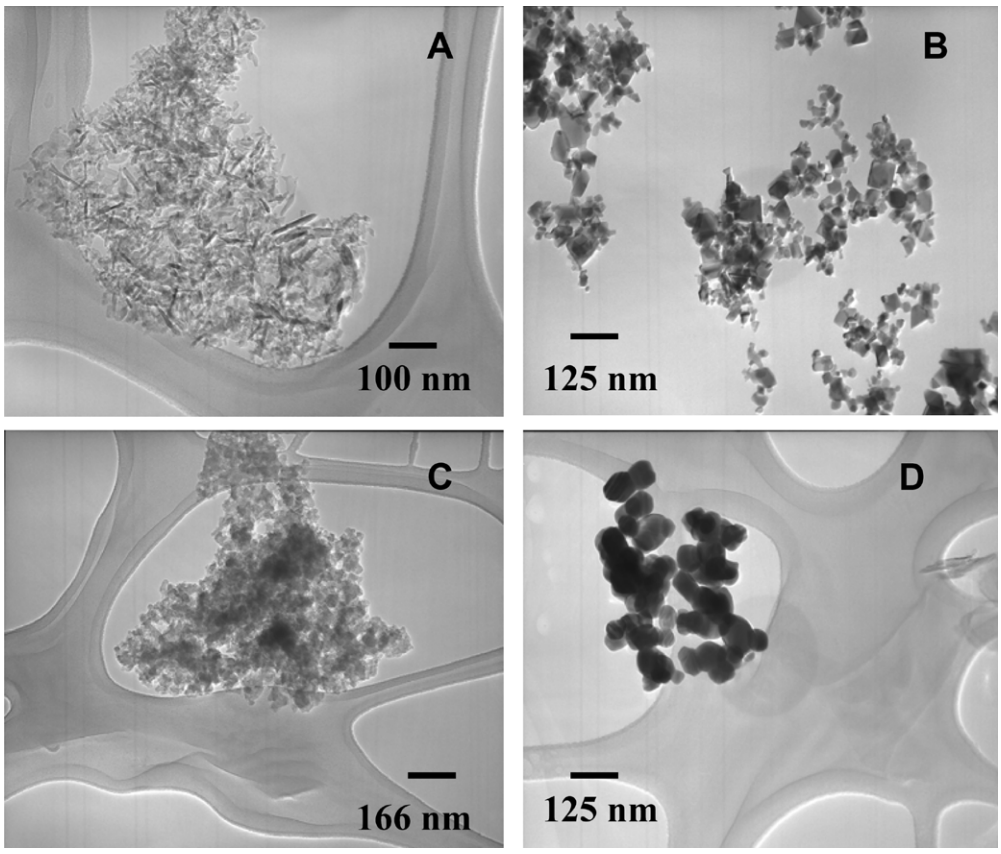

Fig. 1. Transmission electron microscopy images of the investigated nanomaterials: Al_2O_3 (A), CeO_2 (B), SiO_2 (C), and HfO_2 (D).

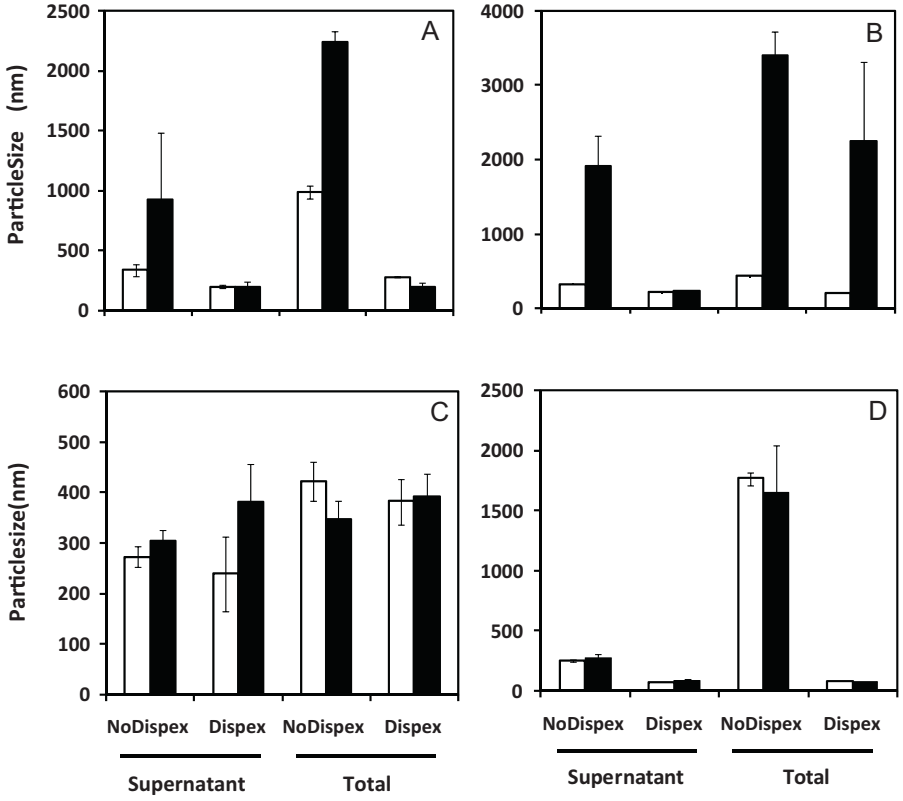

Fig. 2. Effect of dispersant supplementation (100 mg Dispex/L) on the average particle size of different nanoparticles (1000 mg/L), Al_2O_3 (A), CeO_2 (B), SiO_2 (C), and HfO_2 (D), in DI water (□) and in cell-free yeast culture medium (■) following 10 h of incubation (30 °C, 200 rpm). The figure compares the average particle size of the nanomaterials after incubation in the total sample and in the supernatant obtained after allowing dispersions to settle for 30–45 min.

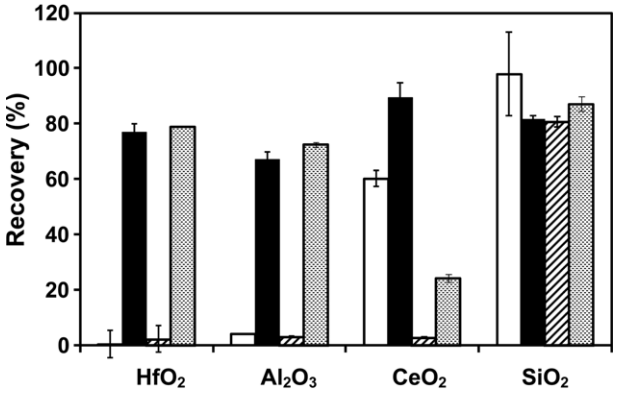

Fig. 3. Effect of dispersant supplementation (100 mg Dispex/L) on the concentration of different nanomaterials (as percentage of the initial concentration in the supernatant) in water and cell-free yeast culture medium following 10 h of incubation (30 °C, 200 rpm). Nanomaterials (1000 mg/L) dispersed in DI water (□), DI water with dispersant (■), yeast culture medium (▨), and yeast culture medium with dispersant (▩). The initial pH of all samples was 6.5. Samples of the supernatant were collected after allowing dispersions to settle for 30–45 min.

structure of the organic compound, and the pH of the dispersions [35].

3.3. Effectiveness of dispersants to promote NP stabilization in yeast culture medium

Two different dispersants, ammonium polyacrylate (Dispex A40) and polyethylemine (PEI), were considered as potential candidates to reduce NP aggregation in YEPD medium. PEI was excluded from further evaluation because the compound was highly inhibitory to yeast at concentrations exceeding 10 mg/L (Fig. 4A). These results are in agreement with previous studies indicating extensive cytotoxicity of PEI to bacteria and various human cell lines [36–38]. In contrast with PEI, Dispex at concentrations up to 100 mg/L was not toxic to yeast (Fig. 4B). Therefore, Dispex concentrations were maintained at concentrations of 100 mg/L or lower in all toxicity tests conducted in this study.

Dispex was an effective dispersing agent for all nanomaterials investigated. As shown in Figs. 2 and 3, a great improvement in HfO_2, Al_2O_3, and CeO_2 dispersion stability was observed upon addition of Dispex (NP/Dispex, 10:1, w/w) in both DI water (pH 6.5) and yeast culture medium. Not only was the average particle size decreased considerably by Dispex addition, but chemical analysis also confirmed that the fraction of inorganic oxides in the supernatant was greatly increased (Fig. 3). As an example, the percentage of Hf, Al, and Ce determined in the supernatant of YEPD medium increased 32, 23 and 8.5-fold, respectively, when the dispersant was added. The effectiveness of Dispex as a dispersant was also confirmed by zeta potential measurements. The value of zeta potential is an index of the relative stability of a dispersion and the degree of repulsion between adjacent particles. A value beyond 30 mV (positive or negative) is often utilized as the arbitrary threshold that separates unstable dispersions with low charged surfaces from stable dispersions with highly charged surfaces [25,39]. The absolute zeta potential values determined for HfO_2, Al_2O_3, and CeO_2 in water (pH 6.5) or yeast culture medium were generally low (see Table S.1 in Supplementary Information), which is in agreement with the high average particle sizes and low fraction of dispersed oxides recorded for those samples. Addition of Dispex to those NP dispersions resulted in highly negative values for the zeta potential (<−27.5 mV), both in pH-6.5 water and YEPD medium (Table S.1), which are indicative of stable dispersions.

3.4. Toxicity of inorganic oxide nanoparticles to yeast

An example of the time course of O_2 consumption in yeast toxicity assays amended with NPs, in this case CeO_2, with and without Dispex is shown in Fig. 5A and B. The O_2 consumption rates in treatments containing NPs were normalized based on the activity of the control treatment lacking NPs and they are plotted as a function of the initial NP concentration in Fig. 5C. In each case, the O_2 oxygen consumption rate was determined during the time period when the control displayed maximum O_2 utilization activity, as shown in the figure.

The inhibition values determined for the various NPs at a concentration of 1000 mg/L are summarized in Table 1. The results obtained indicate that, in the absence of dispersant, the various NPs tested were not inhibitory to *S. cerevisiae* cells at concentrations as high as 1000 mg/L. On the other hand, when the medium was supplemented with dispersant (NP:Dispex, 10:1, w/w), only CeO_2 NPs showed cytotoxicity (46.7% inhibition at 1000 mg/L). O_2-uptake was not inhibited in NP-free controls with Dispex, excluding a possible role of the dispersant in the observed cytotoxicity. Addition of this dispersant led to a considerable increase in the concentration of dispersed CeO_2 in YEPD medium, from 2.9 to 24.3% (Fig. 3); however, it is unclear whether the observed cytotoxicity can be attributed to the enhanced dispersion of CeO_2 or to changes in the surface chemistry of the oxide. The small size of ENM has been suggested to play a critical role in the toxicity of some nanomaterials, and different studies have shown increased cytotoxicity for various NP types with decreasing particle

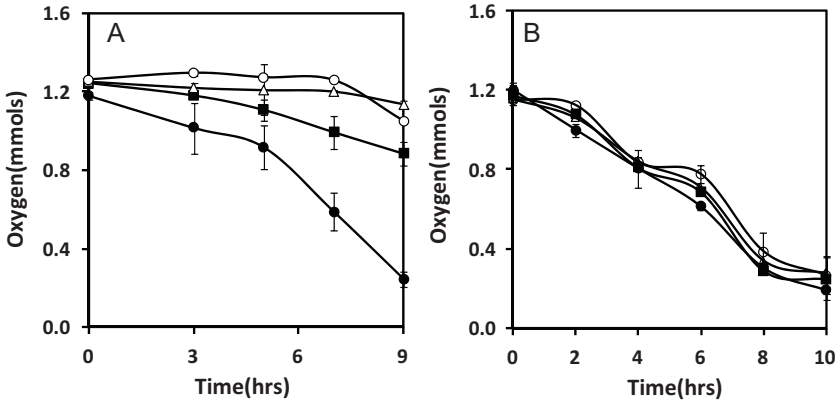

Fig. 4. Consumption of oxygen by *S. cerevisiae* cells as a function of time in assays supplemented with different concentrations of the dispersants polyethylemine (PEI) (Panel A) and ammonium polyacrylate (Dispex) (Panel B). Dispersant concentration (mg/L): 0 (●), 10 (■), 50 (△) and 100 (○).

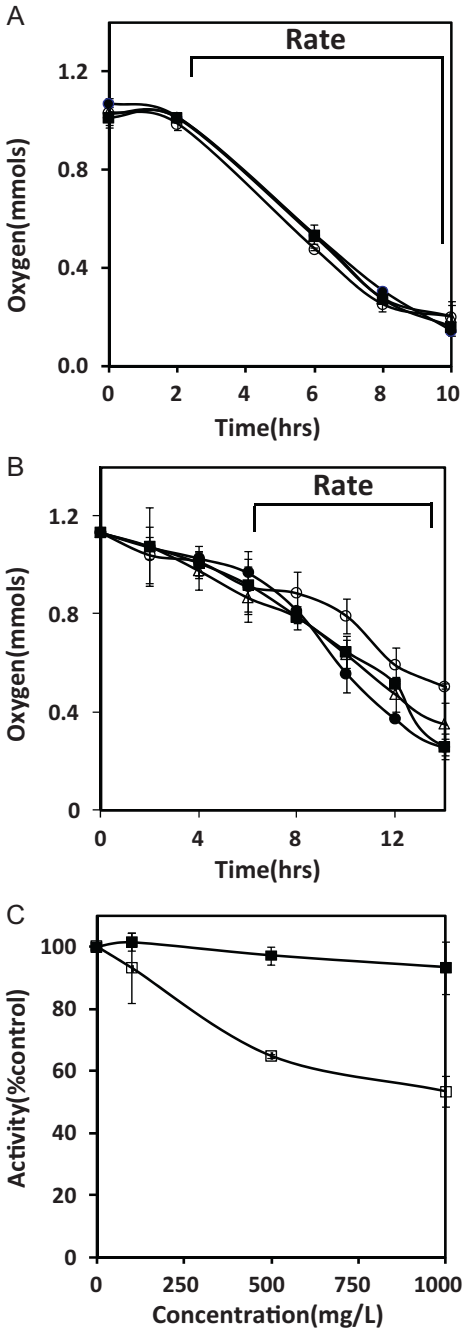

Fig. 5. Consumption of oxygen by *S. cerevisiae* cells as a function of time in assays containing increasing concentrations of nanosized CeO_2 without surfactant (Panel A), and with surfactant supplementation (10:1, NP/surfactant Dispex, w/w) (Panel B): CeO_2 concentrations (mg/L): 0 (●), 100 (■), 500 (△), and 1000 (○). Panels A and B indicate the time period used to determine the O_2 consumption rate. (Panel C) Impact of CeO_2 concentration on the rate of O_2 consumption (as percent of the rate determined in NP-free controls) in assays amended with dispersant (□), and without dispersant (■).

size [40–43]. Based on these premises, enhanced cytotoxicity might be expected for some nanomaterials when effective dispersants are present in the YEPD medium due to their ability to reduce particle agglomeration. Notwithstanding, results from other studies concerned with the impact of dispersants on NP toxicity often fail to demonstrate increased nanotoxicity. Zhang and coworkers (2008) [44] reported that the use of two dispersants, polyethylene glycol and polyvinylpyrrolidone, did not affect much the antibacterial activity of ZnO nanofluids although they

Table 1
Inhibitory effect of different nanosized inorganic oxides (1000 mg/L) on the rate of O_2 consumption by the yeast *S. cerevisiae* in the presence and absence of a dispersant (NPs/Dispex, 10/1, w/w).

Nanoparticles	Inhibition (% control)	
	Without dispersant	With dispersant
CeO_2	6.8 ± 8.5	46.7 ± 4.9
HfO_2	0	0
Al_2O_3	0	0
SiO_2	0	0

enhanced the stability of the suspensions. On the other hand, Cho et al. (2005) [45] demonstrated that the strong antibacterial effects of silver and platinum NPs towards *Staphylococcus aureus* (KCTC 1928) and *E. coli* (KCTC 1041) were negated when the NP dispersions were stabilized by addition of sodium dodecylsulfate.

3.5. Impact of nanoparticles on cell membrane integrity

Flow cytometry analyses were carried out to determine the impact of NP exposure on yeast cell membrane damage. Fig. 6 shows the results obtained in a typical flow cytometry run using yeast cells exposed to NPs under the same conditions utilized in the O_2 consumption inhibition assays. The results presented correspond to cells in a NP-free control and cells exposed to 1000 mg/L of SiO_2 NPs. The figure is divided in four quadrants corresponding to dead cells stained fluorescent red (quadrant R1), compromised cells that are starting to die (R2), live cells with intact membranes which are stained fluorescent green (R3), non-stained cells (R4). Fig. 6B which corresponds to cells exposed to SiO_2 NPs shows a greater number of compromised cells (in R1 and R2) compared to the NP-free control (Fig. 6A), indicating membrane damage by SiO_2 NPs.

Fig. 7 shows the results obtained by flow cytometry analysis for the different NP dispersions at the maximum concentration tested (1000 mg/L). All samples, including the NP-free controls, were incubated with dispersant (100 mg Dispex/L). Flow cytometry assays demonstrated that the dispersant did not cause membrane damage at the concentration used (results not shown). In contrast with the results of O_2-consumption tests which did not show inhibition by SiO_2 and Al_2O_3 NPs at 1000 mg/L, flow cytometry analysis indicated that exposure to both these nanomaterials led to membrane disruption in yeast cells. As shown in Fig. 7, the percentage of cells that did not show membrane damage in the cultures exposed to Al_2O_3 and SiO_2 NPs74.6 and 69.5%, respectively, which is lower compared to the percentage determined in the respective NP-free controls amended with the same concentration of dispersant (88.2%). Lin et al. (2008) [46] observed that exposure of human bronchoalveolar carcinoma-derived cells (A549) to 25 mg/L of nano-sized Al_2O_3 (13–22 nm) led to 83% decrease in cell viability and depolarization of the cell membrane. Exposure of mouse macrophage cells to nanoscale SiO_2 (20 nm) induced a decrease of the membrane fluidity, indicating cell membrane injury [47]. SiO_2 NPs have also been shown to attach to phospholipid bilayers, which is expected to compromise the integrity and functions of the cell membrane [48].

In contrast with SiO_2 and Al_2O_3, exposure to CeO_2 and HfO_2 NPs did not enhance cell membrane damage (Fig. 7). These results suggest that the moderate inhibition of yeast O_2 consumption induced by exposure to CeO_2 NPs did not involve loss of membrane integrity. The underlying mechanisms of CeO_2 toxicity to yeast cells are presently unknown. The cytotoxicity of CeO_2 NPs to human cells [49,50] and freshwater alga [51] has previously been attributed to oxidative stress and lipid peroxidation. However, some studies

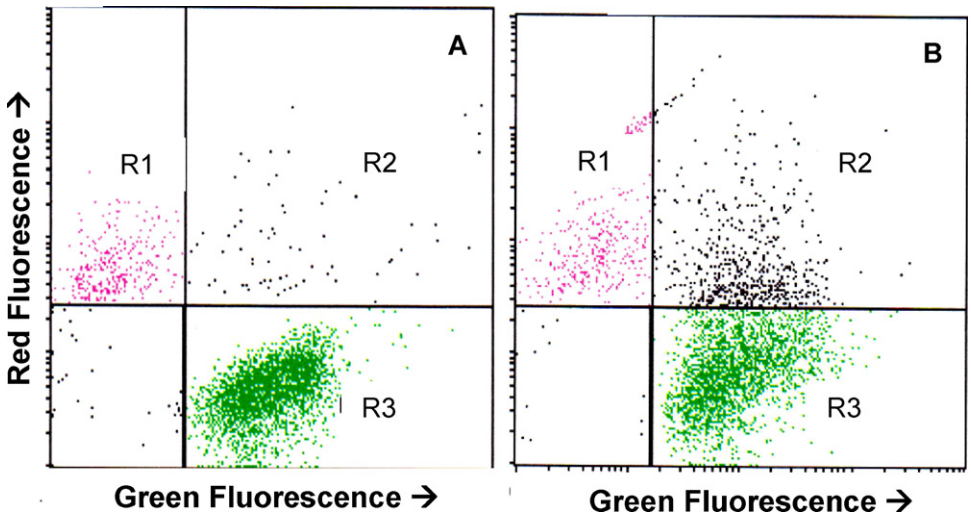

Fig. 6. Flow cytometry analysis of yeast cells exposed to SiO_2 nanoparticles using the dyes, 5-carboxyfluorescein diacetate-acetoxymethyl ester (CFDA-AM, green dye, no membrane damage) and propidium iodide (PI, red dye, membrane damage). Control cells not exposed to SiO_2 (A), and cells exposed to 1000 mg SiO_2/L (B). The quadrant labeled R1 corresponds to non-vital cells (membrane damage), quadrant R2 to vital cells with compromised membrane, quadrant R3 to vital cells with intact membranes, and quadrant R4 to unstained cells. (For interpretation of the references to color in this figure legend, the reader is referred to the web version of the article.)

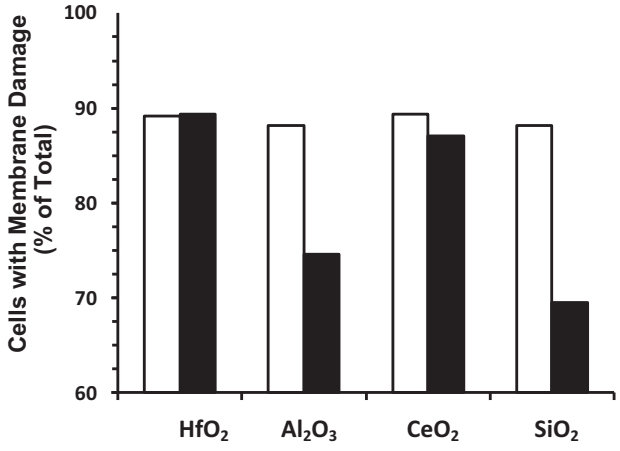

Fig. 7. Impact of exposure to nanosized HfO_2, Al_2O_3, CeO_2, and SiO_2 on the integrity of yeast cells as determined by flow cytometry. Percentage live cells in the nanomaterial-free control (□) and in samples exposed to 1000 mg/L of each nanoscale oxide (■). The percentage of live cells was calculated by subtracting the percentage dead cells and compromised cells from the total. All samples, including the controls, contained dispersant (100 mg Dispex/L).

have demonstrated that nanoscale CeO_2 may also exert antioxidant effects [52–54]. CeO_2 is redox active due to the high standard potential of the redox couple Ce^{IV}/Ce^{III} (above −1.58 V for pH values greater than 1.67) [55]. The toxicity observed in assays with dispersed CeO_2 does not appear to be related to Ce^{III} in the NPs. XPS analysis failed to detect Ce^{III} species on the surface of CeO_2 utilized in this study (see Figure S.1 in Supplementary Information). Furthermore, there was no abiotic O_2 consumption in the assays (see Figure S.2).

4. Conclusions

To our knowledge, this is one of the first systematic studies on effects of inorganic oxide NPs on the eukaryotic cell model organism, *S. cerevisiae*, and the first for evaluation of toxic effects of widely used SiO_2, CeO_2, Al_2O_3 NPs and emerging HfO_2 NPs towards yeast. Dispersed HfO_2, Al_2O_3, and SiO_2 NPs were not toxic to O_2 uptake even when the oxides were supplied at concentrations as high as 1000 mg/L. Exposure to CeO_2 at the same concentration caused 47% inhibition but only if the dispersions were stabilized with a nontoxic polyacrylate dispersant. Flow cytometry analyses confirmed a moderate but significant enhancement in cell membrane damage in yeast cells exposed to dispersed SiO_2 or Al_2O_3 NPs but not in cells exposed to dispersed CeO_2 or HfO_2.

Lastly, this study demonstrates that NPs tend to aggregate in YEPD medium and that, as a result, the effective size of NPs in toxicity bioassays can greatly exceed their primary particle size. A non-toxic dispersant was identified that can be used to enhance the stability of inorganic oxide NPs in yeast culture medium. NP dispersion is a key issue because particle size is believed to determine the cytotoxic activity of some NPs.

Taken as a whole the results of this study demonstrate that nano-sized oxides evaluated, HfO_2, SiO_2, CeO_2, and Al_2O_3, are not expected to be toxic to *S. cerevisiae* cells at environmentally relevant concentrations.

Acknowledgements

This work was supported by a grant of the SRC/Sematech Engineering Research Center for Environmentally Benign Semiconductor Manufacturing. García-Saucedo was funded by CONACyT. Flow cytometry analyses were conducted at the Cytometry Core Facility which is supported by the Cancer Center Support Grant (CCSG-CA-023074).

Appendix A. Supplementary data

Supplementary data associated with this article can be found, in the online version, at doi:10.1016/j.jhazmat.2011.06.081.

References

[1] B.S. Karnik, S.H. Davies, M.J. Baumann, S.J. Masten, Fabrication of catalytic membranes for the treatment of drinking water using combined ozonation and ultrafiltration, Environ. Sci. Technol. 39 (2005) 7656–7661.
[2] M.C. Roco, Nanotechnology: convergence with modern biology and medicine, Curr. Opin. Biotechnol. 14 (2003) 337–346.
[3] F. Gottschalk, T. Sonderer, R.W. Scholz, B. Nowack, Modeled environmental concentrations of engineered nanomaterials (TiO_2, ZnO, Ag, CNT, fullerenes) for different regions, Environ. Sci. Technol. 43 (2009) 9216–9222.

[4] C.O. Hendren, X. Mesnard, J. Dröge, M.R. Wiesner, Estimating production data for five engineered nanomaterials as a basis for exposure assessment, Environ. Sci. Technol. 45 (2011) 2562–2569.
[5] N.C. Mueller, B. Nowack, Exposure modeling of engineered nanoparticles in the environment, Environ. Sci. Technol. 42 (2008) 4447–4453.
[6] R.J. Aitken, M.Q. Chaudhry, A.B.A. Boxall, M. Hull, Manufacture and use of nanomaterials: current status in the UK and global trends, Occup. Med.-Oxford 56 (2006) 300–306.
[7] OECD, List of manufactured nanomaterials and list of end points for phase one of the sponsorship programme for the testing of manufactured nanomaterials: Revision, Organisation for Economic Cooperation and Development, Environment Directorate, Paris. Series on the Safety of Manufactured Nanomaterials No. 27. ENV/JM/MONO(2010)46, 2010.
[8] J.H. Golden, R. Small, L. Pagan, C. Shang, S. Raghavan, Evaluating and treating CMP wastewater, Semicond. Int. 23 (2000) 85–98.
[9] P.H.M. Hoet, I. Brueske-Hohlfeld, O. Salata, Nanoparticles—known and unknown health risks, J. Nanotoxicol. 2 (2004) 1–2.
[10] D.A. Pelletier, A.K. Suresh, G.A. Holton, C.K. McKeown, W. Wang, B.H. Gu, N.P. Mortensen, D.P. Allison, D.C. Joy, M.R. Allison, S.D. Brown, T.J. Phelps, M.J. Doktycz, Effects of engineered cerium oxide nanoparticles on bacterial growth and viability, Appl. Environ. Microbiol. 76 (2010) 7981–7989.
[11] P.A. Zimmerman, B.J. Rice, E.C. Piscani, V. Liberman, High index 193 nm immersion lithography: the beginning or the end of the road, in: H.J. Levinson, M.V. Dusa (Eds.), Optical Microlithography XXII, vol. 7274, Society of Photo-optical Instrumentation Engineers (SPIE), San Jose, CA, USA, 2009, p. 727420.
[12] W.J. Bae, M. Trikeriotis, J. Sha, E.L. Schwartz, R. Rodriguez, P. Zimmerman, E.P. Giannelis, C.K. Ober, High refractive index and high transparency HfO_2 nanocomposites for next generation lithography, J. Mater. Chem. 20 (2010) 5186–5189.
[13] J.M. Balbus, A.D. Maynard, V.L. Colvin, V. Castranova, G.P. Daston, R.A. Denison, K.L. Dreher, P.L. Goering, A.M. Goldberg, K.M. Kulinowski, N.A. Monteiro-Riviere, G. Oberdorster, G.S. Omenn, K.E. Pinkerton, K.S. Ramos, K.M. Rest, J.B. Sass, E.K. Silbergeld, B.A. Wong, Meeting report: hazard assessment for nanoparticles—report from an interdisciplinary workshop, Environ. Health Perspect. 115 (2007) 1654–1659.
[14] M.R. Gwinn, V. Vallyathan, Nanoparticles: health effects—pros and cons, Environ. Health Perspect. 114 (2006) 1818–1825.
[15] R.D. Handy, F. von der Kammer, J.R. Lead, M. Hassellov, R. Owen, M. Crane, The ecotoxicology and chemistry of manufactured nanoparticles, Ecotoxicology 17 (2008) 287–314.
[16] S.J. Klaine, P.J.J. Alvarez, G.E. Batley, T.F. Fernandes, R.D. Handy, D.Y. Lyon, S. Mahendra, M.J. McLaughlin, J.R. Lead, Nanomaterials in the environment: behavior, fate, bioavailability, and effects, Environ. Toxicol. Chem. 27 (2008) 1825–1851.
[17] B. Nowack, T.D. Bucheli, Occurrence, behavior and effects of nanoparticles in the environment, Environ. Pollut. 150 (2007) 5–22.
[18] G. Oberdorster, V. Stone, K. Donaldson, Toxicology of nanoparticles: a historical perspective, Nanotoxicology 1 (2007) 2–25.
[19] W.G. Kreyling, M. Semmler-Behnke, W. Moller, Health implications of nanoparticles, J. Nanopart. Res. 8 (2006) 543–562.
[20] L.K. Limbach, Y.C. Li, R.N. Grass, T.J. Brunner, M.A. Hintermann, M. Muller, D. Gunther, W.J. Stark, Oxide nanoparticle uptake in human lung fibroblasts: effects of particle size, agglomeration, and diffusion at low concentrations, Environ. Sci. Technol. 39 (2005) 9370–9376.
[21] M. Auffan, J. Rose, J.Y. Bottero, G.V. Lowry, J.P. Jolivet, M.R. Wiesner, Towards a definition of inorganic nanoparticles from an environmental, health and safety perspective, Nat. Nanotechnol. 4 (2009) 634–641.
[22] A. Kroll, M.H. Pillukat, D. Hahn, J. Schnekenburger, Current in vitro methods in nanoparticle risk assessment: limitations and challenges, Eur. J. Pharm. Biopharm. 72 (2009) 370–377.
[23] V. Rabolli, L.C.J. Thomassen, C. Princen, D. Napierska, L. Gonzalez, M. Kirsch-Volders, P.H. Hoet, F. Huaux, C.E.A. Kirschhock, J.A. Martens, D. Lison, Influence of size, surface area and microporosity on the in vitro cytotoxic activity of amorphous silica nanoparticles in different cell types, Nanotoxicology 4 (2010) 307–318.
[24] G. Oberdörster, A. Maynard, K. Donaldson, V. Castranova, J. Fitzpatrick, K. Ausman, J. Carter, B. Karn, W. Kreyling, D. Lai, S. Olin, N. Monteiro-Riviere, D. Warheit, H. Yang, Principles for characterizing the potential human health effects from exposure to nanomaterials: elements of a screening strategy, Part. Fibre Toxicol. 2 (2005) 8.
[25] R.C. Murdock, L. Braydich-Stolle, A.M. Schrand, J.J. Schlager, S.M. Hussain, Characterization of nanomaterial dispersion in solution prior to in vitro exposure using dynamic light scattering technique, Toxicol. Sci. 101 (2008) 239–253.
[26] A. Buschini, P. Poli, C. Rossi, Saccharomyces cerevisiae as an eukaryotic cell model to assess cytotoxicity and genotoxicity of three anticancer anthraquinones, Mutagenesis 18 (2003) 25–36.
[27] M.G. Cabral, C.A. Viegas, M.C. Teixeira, I. Sa-Correia, Toxicity of chlorinated phenoxyacetic acid herbicides in the experimental eukaryotic model *Saccharomyces cerevisiae*: role of pH and of growth phase and size of the yeast cell population, Chemosphere 51 (2003) 47–54.
[28] M. Schmitt, G. Gellert, J. Ludwig, H. Lichtenberg-Frate, Phenotypic yeast growth analysis for chronic toxicity testing, Ecotoxicol. Environ. Safety 59 (2004) 142–150.
[29] J. Schwegmann, A.J. Feitz, F.H. Frimmel, Influence of the zeta potential on the sorption and toxicity of iron oxide nanoparticles on *S. cerevisiae* and *E. coli*, J. Colloid Interface Sci. 347 (2010) 43–48.
[30] K. Kasemets, A. Ivask, H.C. Dubourguier, A. Kahru, Toxicity of nanoparticles of ZnO, CuO and TiO_2 to yeast *Saccharomyces cerevisiae*, Toxicol. in Vitro 23 (2009) 1116–1122.
[31] A.N. Hadduck, V. Hindagolla, A.E. Contreras, Q.L. Li, A.T. Bakalinsky, Does aqueous fullerene inhibit the growth of *Saccharomyces cerevisiae* or *Escherichia coli*? Appl. Environ. Microbiol. 76 (2010) 8239–8242.
[32] APHA, in: L.S. Clesceri, et al. (Eds.), Standard Methods for the Examination of Water and Wastewater, 20th ed., American Public Health Association, Washington, DC, 1998.
[33] M. Kosmulski, Chemical Properties of Material Surfaces, Marcel Dekker, 2001.
[34] P. Blanc, A. Larbot, L. Cot, Hafnia colloidal solution from hydrothermal synthesis and membrane preparation, J. Eur. Ceram. Soc. 3 (1997).
[35] R.D. Handy, R. Owen, E. Valsami-Jones, The ecotoxicology of nanoparticles and nanomaterials: current status, knowledge gaps, challenges, and future needs, Ecotoxicology 17 (2008) 315–325.
[36] A.C. Hunter, Molecular hurdles in polyfectin design and mechanistic background to polycation induced cytotoxicity, Adv. Drug Deliv. Rev. 58 (2006) 1523–1531.
[37] L. Peng, Y. Gao, Y.N. Xue, S.W. Huang, R.X. Zhuo, Cytotoxicity and in vivo tissue compatibility of poly(amidoamine) with pendant aminobutyl group as a gene delivery vector, Biomaterials 31 (2010) 4467–4476.
[38] J. Robbens, C. Vanparys, I. Nobels, R. Blust, K. Van Hoecke, C. Janssen, K. De Schamphelaere, K. Roland, G. Blanchard, F. Silvestre, V. Gillardin, P. Kestemont, R. Anthonissen, O. Toussaint, S. Vankoningsloo, C. Saout, E. Alfaro-Moreno, P. Hoet, L. Gonzalez, P. Dubruel, P. Troisfontaines, Eco-, geno- and human toxicology of bio-active nanoparticles for biomedical applications, Toxicology 269 (2010) 170–181.
[39] Anonymous, Zetasizer Nano Series User Manual. MAN0317 Issue 2.2, Malvern Instruments Ltd., Worcestershire, UK, 2005.
[40] W. Liu, Y. Wu, C. Wang, H.C. Li, T. Wang, C.Y. Liao, L. Cui, Q.F. Zhou, B. Yan, G.B. Jiang, Impact of silver nanoparticles on human cells: effect of particle size, Nanotoxicology 4 (2010) 319–330.
[41] S. Makhluf, R. Dror, Y. Nitzan, Y. Abramovich, R. Jelinek, A. Gedanken, Microwave-assisted synthesis of nanocrystalline MgO and its use as a bacteriocide, Adv. Funct. Mater. 15 (2005) 1708–1715.
[42] O. Yamamoto, Influence of particle size on the antibacterial activity of zinc oxide, Int. J. Inorg. Mater. 3 (2001) 643–646.
[43] S. Nair, A. Sasidharan, V.V.D. Rani, D. Menon, K. Manzoor, S. Raina, Role of size scale of ZnO nanoparticles and microparticles on toxicity toward bacteria and osteoblast cancer cells, J. Mater. Sci.-Mater. Med. 20 (2009) 235–241.
[44] L.L. Zhang, Y.H. Jiang, Y.L. Ding, M. Povey, D. York, Investigation into the antibacterial behaviour of suspensions of ZnO nanoparticles (ZnO nanofluids), J. Nanopart. Res. 9 (2007) 479–489.
[45] K.H. Cho, J.E. Park, T. Osaka, S.G. Park, The study of antimicrobial activity and preservative effects of nanosilver ingredient, Electrochim. Acta 51 (2005) 956–960.
[46] W. Lin, I. Stayton, Y.-W. Huang, X.-D. Zhou, Y. Ma, Cytotoxicity and cell membrane depolarization induced by aluminum oxide nanoparticles in human lung epithelial cells A549, Toxicol. Environ. Chem. 90 (2008) 983–996.
[47] H. Yang, Q.Y. Wu, M. Tang, L. Kong, Z.H. Lu, Cell membrane injury induced by silica nanoparticles in mouse macrophage, J. Biomed. Nanotechnol. 5 (2009) 528–535.
[48] H. Jang, L.E. Pell, B.A. Korgel, D.S. English, Photoluminescence quenching of silicon nanoparticles in phospholipid vesicle bilayers, J. Photochem. Photobiol. A: Chem. 158 (2003) 111–117.
[49] E.-J. Park, J. Choi, Y.-K. Park, K. Park, Oxidative stress induced by cerium oxide nanoparticle in cultured BEAS-2B cells, Toxicology 245 (2008) 90–100.
[50] M. Auffan, J. Rose, T. Orsiere, M. De Meo, A. Thill, O. Zeyons, O. Proux, A. Masion, P. Chaurand, O. Spalla, A. Botta, M.R. Wiesner, J.Y. Bottero, CeO_2 nanoparticles induce DNA damage towards human dermal fibroblasts in vitro, Nanotoxicology 3 (2009) 161–171.
[51] N.J. Rogers, N.M. Franklin, S.C. Apte, G.E. Batley, B.M. Angel, J.R. Lead, M. Baalousha, Physico-chemical behaviour and algal toxicity of nanoparticulate CeO_2 in freshwater, Environ. Chem. 7 (2009) 50–60.
[52] T. Xia, M. Kovochich, M. Liong, L. Mädler, B. Gilbert, H. Shi, J.I. Yeh, J.I. Zink, A.E. Nel, Comparison of the mechanism of toxicity of zinc oxide and cerium oxide nanoparticles based on dissolution and oxidative stress properties, ACS Nano 2 (2008) 2121–2134.
[53] D. Schubert, R. Dargusch, J. Raitano, S.W. Chan, Cerium and yttrium oxide nanoparticles are neuroprotective, Biochem. Biophys. Res. Commun. 342 (2006) 86–91.
[54] J. Chen, S. Patil, S. Seal, J.F. McGinnis, Rare earth nanoparticles prevent retinal degeneration induced by intracellular peroxides, Nat. Nanotechnol. 1 (2006) 142–150.
[55] A.S. Karakoti, S. Kuchibhatla, K.S. Babu, S. Seal, Direct synthesis of nanoceria in aqueous polyhydroxyl solutions, J. Phys. Chem. C 111 (2007) 17232–17240.